# Vector optical activity in the Weyl semimetal TaAs

M. R. Norman

# Vector Optical Activity in the Weyl Semimetal TaAs

M. R. Norman[1]

[1]*Materials Science Division, Argonne National Laboratory, Argonne, IL 60439, USA*
(Dated: December 10, 2015)

It is shown that the Weyl semimetal TaAs can have a significant polar vector contribution to its optical activity. This is quantified by ab initio calculations of the resonant x-ray diffraction at the Ta L1 edge. For the Bragg vector (400), this polar vector contribution to the circular intensity differential between left and right polarized x-rays is predicted to be comparable to that arising from linear dichroism, which could be tested by future experiments. Implications this result has in regards to optical effects predicted for topological Weyl semimetals are discussed.

PACS numbers: 78.70.Ck, 78.20.Ek, 75.70.Tj

Weyl semimetals are predicted to have a variety of novel optical effects due to their topological electronic structure [1–4]. But in the case of Weyl semimetals which exist because of inversion symmetry breaking, unusual optical effects can also arise depending on the space group of the lattice. Disentangling these two sources will be important in order to ascertain which effects arise due to such phenomena as the axial anomaly, and which are simply due to the influence of the crystallography on the electronic structure.

Recently, much attention has focused on the Weyl semimetal TaAs where unusual Fermi arc surface states have been observed by photoemission [5, 6] as predicted by theory [7, 8]. These and related materials also show novel magnetoresistance phenomena, including evidence for the axial anomaly [9, 10] predicted long ago by Nielsen and Ninomiya [11]. This axial anomaly can also cause circular dichroism and related chiral optical effects [1–4].

Of course, multiferroics can also exhibit similar optical effects, but perhaps more relevant for the case of TaAs, chiral crystal structures can as well. For the latter, these are reciprocal (natural) optical activity, as opposed to non-reciprocal activity due to time reversal symmetry breaking. This requires the breaking of inversion symmetry. Depending on the space group, a variety of effects can be observed, and this was spelled out in a classic paper by Jerphagnon and Chemla [12]. The gyration tensor has nine elements that can be decomposed in terms of a pseudoscalar, a polar vector, and a symmetric traceless second rank tensor known as a pseudodeviator. The pseudoscalar is responsible for natural circular dichroism in the optical frequency range due to interference between the electric dipole and magnetic dipole scattering terms (E1-M1). The pseudodeviator is responsible for natural circular dichroism in the x-ray regime (XNCD) due to interference between the electric dipole and electric quadrupole scattering terms (E1-E2) [13].

The second, polar vector contribution, does not lead to optical activity in the traditional sense, but it does lead to the generation of a longitudinal electric field in the sample [12]. This field, though, is predicted to be small and thus difficult to observe. But long ago, Voigt [14]

and Fedorov [15] realized this this could lead to polarization rotation in the reflected light for incoming light not along the normal to the surface. In 1978, this effect was reported for CdS [16, 17]. A general theory for this and related optical effects was worked out by Graham and Raab [18]. A related polarization rotation has been observed in the x-ray regime at the Zn K edge for ZnO [19].

An important point about CdS, ZnO, and related materials is that only the polar vector contribution is present. Interestingly, the $I4_1md$ space group for TaAs and its relatives (TaP, NbAs, NbP) also has this property [20]. This is of particular relevance since similar optical effects have been discussed by Kargarian *et al.* [3] that are connected with the Fermi surface arc states which are known to be present in TaAs. In one of their geometries where the surface contains Fermi arcs, they predict the generation of a longitudinal electric field. As commented by this author [20], for oblique incidence, one would also expect polarization rotation in the reflected light as in CdS. Differentiating their topological effect from the crystallographic effect could be a challenge in materials like TaAs.

To get a handle on the latter, we turn to ab initio work. Although the calculation of optical spectra is very sensitive to the assumed band structure, this simplifies considerably in the x-ray regime. As in the work done on ZnO [19], the approach is to find the optimal conditions to detect the polar vector contribution to guide future experiments. To see this, we first outline the geometry of such experiments in Fig. 1. Here, the surface normal defines the scattering vector, $Q$, which is the difference of the outgoing wavevector $k_o$ and the incoming wavevector $k_i$. $\theta$ is the Bragg angle which is the angle of $k_i$ relative to the surface (so an angle of 90° corresponds to normal incidence). $\psi$ is the azimuthal angle for rotation about $Q$. $\psi = 0°$ corresponds to the incidence plane being defined by $Q$ and $I$, with $I \equiv z$ for $Q$ along $x$, where $z$ is the optical axis (the $c$ axis in the case of TaAs). Note that the electric polarization vector for $\sigma$ polarization is perpendicular to the incidence plane, whereas for $\pi$
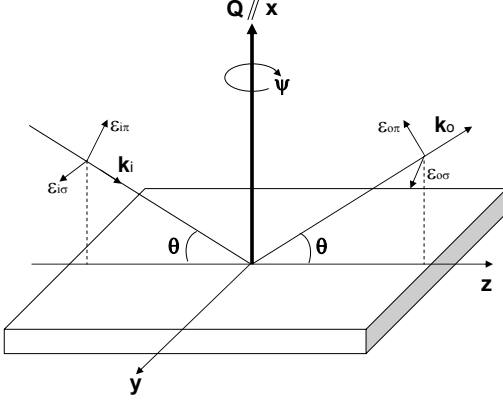
FIG. 1: Scattering geometry, with $k_i$ the incident wavevector, $k_o$ the outgoing one, and the scattering vector $Q$ is normal to the surface. $\theta$ is the Bragg angle, $\psi$ the azimuthal angle, and $\epsilon$ denotes the polarization. The geometry shown is for $Q$ along $x$, with the optical ($c$) axis along $z$.

polarization it is in this plane.

To get at the polar vector optical activity contribution, one can look at the so-called x-ray circular intensity differential (XCID) which is the difference of scattering intensity between left polarized incoming x-rays ($L$) and right polarized incoming x-rays ($R$). With no analysis of the outgoing polarization, this can be written as [19]:

$$I^L - I^R = -2\text{Im}[f^{\sigma\sigma}(f^{\pi\sigma})^* + f^{\sigma\pi}(f^{\pi\pi})^*] \quad (1)$$

where $f$ is the elastic scattering factor, with the first index denoting incoming polarization, and the last outgoing polarization. Note that $f$ is

$$f \equiv \sum_n e^{iQ\cdot r_n} f_n \quad (2)$$

where $n$, the site index, is implicit in the following. The scattering factor $f$ is a sum of the Thomson scattering, and then various terms corresponding for resonant scattering to excitations from a core orbital to unoccupied valence orbitals and then back again [21]. That is, the scattering matrix elements, $< M|\hat{O}^*|N >< N|\hat{O}|M >$ (where $M$ is the ground state and $N$ the excited state) can be expanded in a multipole series since for the relevant Hamiltonian ($\hat{H}$) terms, up to quadrupolar order, $\hat{O} \equiv \epsilon\cdot r(1+\frac{i}{2}k\cdot r)$ where $k$ is the wavevector and $\epsilon$ the polarization. This leads to the dipole (E1) contribution $\epsilon\cdot r$ and the quadrupole (E2) contribution $\frac{i}{2}(k\cdot r)(\epsilon\cdot r)$, giving rise in $f$ to dipole terms (E1-E1), quadrupole terms (E2-E2), and dipole-quadrupole interference terms (E1-E2), the last existing only if the site $n$ does not have inversion symmetry. Here, additional magnetic dipole terms coming from $\hat{H}$ have been dropped since they are negligible in the x-ray regime, as well as higher order (octupole, etc.) terms in the multipole expansion.

As discussed by Graham and Raab [18], the desired polar vector effect cannot be observed by XCID with $Q$ along the optic axis, though a related intensity differential can occur (see below). Instead, we first turn to the case when $Q$ is along the $x$ direction as in the work on ZnO [19], where by $x$ we mean along the tetragonal $a$ axis.

For the polar vector contribution to the optical activity, the crucial term is the E1-E2 contribution to the scattering factors $f^{\sigma\pi}$ and $f^{\pi\sigma}$, which was shown by Goulon et al. [19] for the point group 6mm and $Q$ along $x$ to be proportional to $\sin(2\theta)\sin(\psi)t_{xxz}$ where

$$t_{\alpha\beta\gamma} \equiv < M|r_\alpha|N >< N|r_\beta r_\gamma|M > \quad (3)$$

which can be easily derived from the functional form for E1-E2 [19, 21]

$$f_{E1-E2} = \frac{i}{2}\sum_N \frac{(E_M - E_N)^2}{E_M - E_N + \omega + i\Gamma/2} \quad (4)$$
$$\sum_{\alpha\beta\gamma} \epsilon_{o\alpha}^*\epsilon_{i\beta}(t_{\alpha\beta\gamma}k_{i\gamma} - t_{\beta\alpha\gamma}^*k_{o\gamma})$$

where $E_M$ and $E_N$ are the energies of the ground and excited states, respectively, and $\Gamma$ the inverse lifetime of the excited state (here, $\hbar$ and the electron mass $m$ have been set to 1). This contribution (zero for $\sigma\sigma$ and $\pi\pi$) is invariant under interchange of $\sigma$ and $\pi$ indices. On the other hand, there are dipole (E1-E1) and quadrupole (E2-E2) contributions to these two scattering factors as well (noting that $f^{\sigma\sigma}$ and $f^{\pi\pi}$ are dominated by the large Thomson scattering term which does not contribute to $f^{\sigma\pi}$ and $f^{\pi\sigma}$). The dipole one

$$f_{E1-E1} = \sum_N \frac{(E_M - E_N)^2}{E_M - E_N + \omega + i\Gamma/2}\sum_{\alpha\beta} \epsilon_{o\alpha}^*\epsilon_{i\beta}d_{\alpha\beta} \quad (5)$$

goes as $\sin(\theta)\sin(2\psi)(d_{zz} - d_{xx})$ where

$$d_{\alpha\beta} \equiv < M|r_\alpha|N >< N|r_\beta|M > \quad (6)$$

with this contribution being odd under the interchange of $\sigma$ and $\pi$ indices. The more complicated quadrupole (E2-E2) term instead involves the azimuthal factor $\sin(4\psi)$. These forms can be easily shown to apply to the 4mm point group of TaAs as well. Because of the differing azimuthal factors of these three terms, they can be differentiated by performing an azimuthal sweep. In particular, for an azimuthal angle of 90° (that is, with the $c$ axis perpendicular to the incidence plane), the E1-E1 and E2-E2 terms vanish, and the XCID is determined by the polar vector E1-E2 contribution.

Based on the above, to maximize this polar vector contribution, one wants Bragg angles near 45° [19]. At the Ta L1 edge, the Bragg vector (400) ($2\pi/a$ units) has a Bragg angle of 38.1°, close to the desired value. To proceed, we turn to ab initio work, employing the multiple
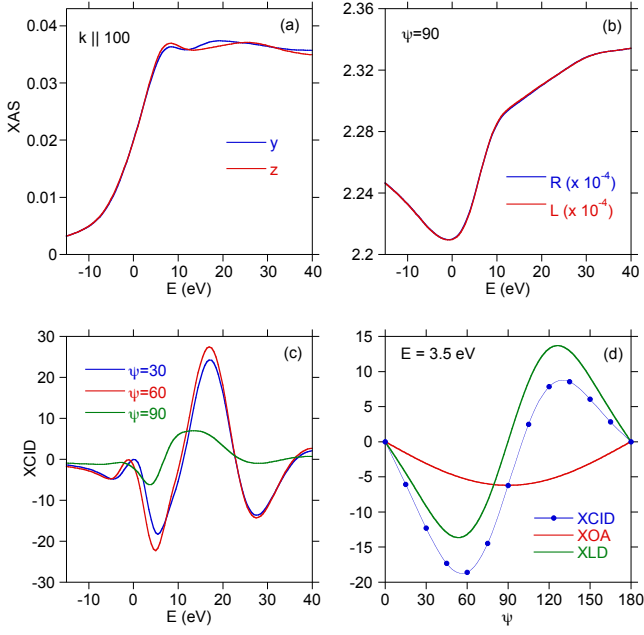
FIG. 2: (Color online) Ta L1 edge - (a) X-ray absorption (XAS) for $k$ along (100) for electric polarizations parallel to $y$ and $z$. (b) Resonant x-ray scattering intensity for incoming left (L) and right (R) polarized x-rays for a Bragg vector (400) and an azimuthal angle of 90°. (c) XCID intensity (L - R) for three azimuthal angles. (d) XCID intensity and corresponding decomposition into XLD and XOA contributions at an energy of 3.5 eV. The unit for absorption is Mbarn, and for scattering intensities number of electrons squared (summed over the unit cell). The zero of energy is at 11.682 keV.

FIG. 3: (Color online) Ta L1 edge - Comparison of XLD $(y-z)$ and XCID for an azimuthal angle of (a) 45° and (b) 90°. (c) Resonant x-ray intensities for various azimuthal angles, with the first polarization index for incoming x-rays, the second for outgoing x-rays. (d) Difference of the two intensities in (c) for an azimuthal angle of 45° (for 90°, the difference is zero).

scattering Greens function code FDMNES [22] including spin-orbit interactions [23]. The simulations were done using local density (LDA) atomic potentials (Hedin-Lundqvist exchange-correlation function) in a muffin tin approximation that considers multiple scattering of the photoelectron around the absorbing site [24]. The cluster radius is limited by the photoelectron lifetime [25]. For the present case (Ta L1 edge), the results for cluster radii of 5 Å and 6 Å are similar, indicating cluster convergence. Results shown are for a radius of 6 Å, which corresponds to 55 atoms around the Ta site.

Fig. 2a shows the x-ray absorption spectrum for TaAs at the L1 edge. From this plot, one can see that the x-ray linear dichroism for this material is predicted to be weak. The resulting resonant x-ray scattering intensity for the Bragg vector (400) is shown in Fig. 2b for incoming right and left polarized light (summed over outgoing polarizations). Again, these two spectra are almost identical since the scattering is dominated by the Thomson scattering term which is large for Ta, which has a large $Z$. Subtracting the two polarizations, one obtains the x-ray circular intensity differential (XCID) shown in Fig. 2c for several representative azimuthal angles. The spectra for 30° and 60° are similar, but the one for 90° is different.
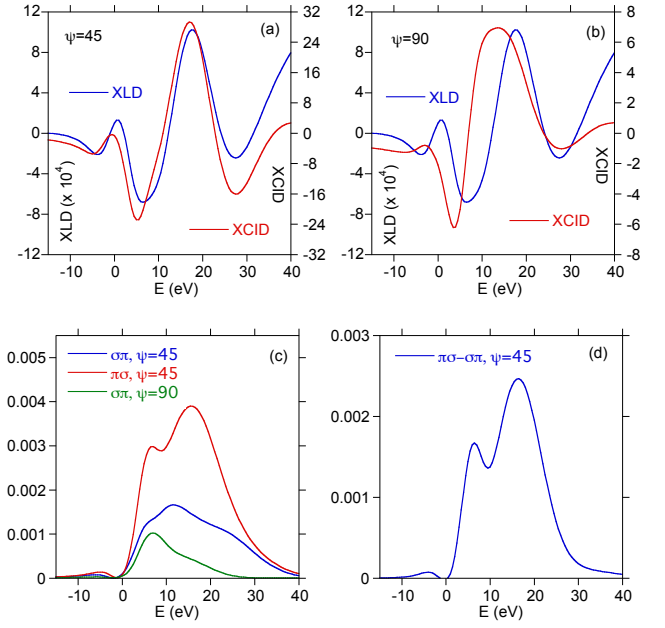
For a representative energy, the azimuthal dependence of the intensity is plotted in Fig. 2d. This can be fit by the sum of three terms, one going as $\sin(\psi)$, the others as $\sin(2\psi)$ and $\sin(4\psi)$. The latter two are due to the E1-E1 and E2-E2 terms and are related to the x-ray linear dichroism (XLD), as shown more explicitly in Fig. 3a for an azimuthal angle of 45°. The first, though, is due to the desired x-ray optical activity (XOA) coming from the E1-E2 interference term $t_{xxz}$. This term determines the XCID at an azimuthal angle of 90° as seen in Fig. 2d and illustrated further in Fig. 3b. For a general azimuthal angle, the XOA contribution is predicted to be significant compared to the XLD contribution, as contrasted with ZnO at the Zn K edge [19]. On the other hand, in absolute numbers, the XOA term is small, of order 0.03% of the total scattering intensity shown in Fig. 2b.

This brings us to the question of whether there is something else besides the XCID that could be exploited. The answer is yes if one has control over both incoming polarization and measuring outgoing polarization. The reason is that the Thomson scattering does not contribute to the $\sigma\pi$ and $\pi\sigma$ terms. In Fig. 3c, the scattering intensity for these polarization settings are shown for two representative azimuthal angles. Again, for 90°, the total contribution is due to the XOA one, with the large difference in the two polarization settings for 45° due to the XOA term (Figs. 3c and 3d).

So, what about Bragg vectors along the $c$ axis? Calculations have also been done at the Ta M1 edge for $Q$=(004) ($2\pi/c$ units). As discussed by Graham and Raab [18], one way to get at the polar vector term in this case is to look at incoming light (either $L$ or $R$), but measuring the outgoing light for 45° and -45° polarizations and taking the difference (with $\pi$ corresponding to 0° and $\sigma$ to 90°). This is challenging, since as in the previous paragraph, it requires exquisite control of the incoming polarization and measuring the outgoing one. But if one calculates the azimuthal dependence, one finds that both the E1-E1 and E1-E2 contributions do not depend on azimuthal angle in this geometry, and therefore it is the quadrupole terms that solely drives this dependence (which is predicted to be weak). Therefore, although XOA does exist for this geometry, it would be difficult to quantify experimentally, which can be traced to the fact that in this geometry, the $\sigma\pi$ and $\pi\sigma$ terms vanish identically [18, 26].

We now turn to the implications our results have in regards to optical activity due to the topological properties of this material, which played no role in the above calculations. This has been treated most definitively by Kargarian *et al.* [3]. To make connection to this work, let us summarize what would be expected for optical activity due to crystallographic effects (Table 1). For the point group relevant for TaAs, a longitudinal electric field inside the sample is expected for light propagating along the $x$ ($a$) axis and polarization along the $z$ ($c$) axis due to the polar vector optical activity [12]. This can be easily seen since in this case, the only non-zero terms of the gyration tensor are $g_{yx} = -g_{xy}$. This is analogous to the longitudinal electric field discussed by Kagarian *et al.* [3] in a geometry where the surface contains Fermi arcs. The associated optical activity can be determined by reflection if the incidence wavevector is not along the surface normal. According to Graham and Raab [18], this shows up as a polarization rotation if the optic axis ($c$ axis in the present case) is in the surface and also not in the incidence plane (that is $\psi$ not equal to 0° or 180° in the geometry of Fig. 1). The analogous XOA results are shown in Figs. 2 and 3. These XOA effects also contribute to $\sigma\sigma$ and $\pi\pi$ if the optic axis instead is along the surface normal, but as discussed in the previous section, they are not easily separated from the ordinary dipole contribution since neither depends on the azimuthal angle. Interestingly, this is exactly the surface for TaAs that contains Fermi arcs [5–8]. For the geometry appropriate to Figs. 2 and 3 (that is, with the surface normal along the $a$ axis), the situation is less clear, since such a surface may or may not contain Fermi arcs [8], and the evidence from photoemission either way is not clear [5]. Certainly, we anticipate that what is due to crystallography, and what is due to the topological electronic structure, may be difficult to separate.

On the other hand, if the topological effect is due to

TABLE I: Summary of vector optical activity effects in TaAs in reflection geometry (Fig. 1), with the first column the reflection plane (crystal surface), the second the non-zero polar vector reflection terms, and the third the azimuthal dependence. In the first row, the polar vector contribution can be extracted by using incoming circular light and measuring the difference of the outgoing light for 45° and -45° polarizations [18]. For the second row, $\psi$=0 corresponds to the $z$ ($c$) axis being in the incidence plane. For this $yz$ surface, the polar vector term can also be extracted by looking at the difference of right and left polarized light. Details and caveats are described in the text.

| surface | reflection terms | azimuthal dependence |
| --- | --- | --- |
| $xy$ | $\sigma\sigma$, $\pi\pi$ | none |
| $yz$ | $\sigma\pi$, $\pi\sigma$ | $\sin(\psi)$ |

time reversal breaking [3], then the two effects can in principle be distinguished by applying a magnetic field. An analogous effect has been demonstrated in tellurium, which is also thought to be topological in nature [27]. At zero field, polarization rotation occurs for transmitted light due to fact that the space group breaks inversion symmetry (with both natural optical activity and XNCD allowed [20]), but the application of a current leads to an additional polarization rotation due to time reversal breaking [28]. Such a Faraday rotation is predicted by Kargarian *et al.* [3] for a surface which does not contain Fermi arcs, but interestingly no optical rotation would occur in TaAs due to crystallography since its space group does not allow for natural optical activity (unlike tellurium) [20]. So, in this case, any polarization rotation of the transmitted light should be topological in nature.

In summary, Weyl semimetals can exhibit optical activity due both to its topological electronic structure, and to crystallography. By constructing experiments where the latter effect is minimized, the unique topological signatures can be identified. Regardless, the novel Weyl semimetal TaAs, as well as its related siblings (TaP, NbAs, NbP), should exhibit novel optical activity of a polar vector nature that in principle can be identified by appropriate resonant x-ray diffraction measurements, as demonstrated here.

*Note added.* Recently, a paper appeared predicting a quantum nonlinear Hall effect induced by the dipole of the Berry curvature [29]. The condition for the existence of the antisymmetric part of this dipole is the same as that for the vector optical activity.

[1] P. Hosur and X.-L. Qi, Phys. Rev. B **91**, 081106(R) (2015).

[2] P. Goswami, G. Sharma and S. Tewari, Phys. Rev. B **92**, 161110(R) (2015).

[3] M. Kargarian, M. Randeria and N. Trivedi, Sci. Rep. **5**, 12683 (2015).

[4] S. Zhong, J. Orenstein and J. E. Moore, Phys. Rev. Lett. **115**, 117403 (2015).

[5] S.-Y. Xu, I. Belopolski, N. Alidoust, M. Neupane, G. Bian, C. Zhang, R. Sankar, G. Chang, Z. Yuan, C.-C. Lee, S.-M. Huang, H. Zheng, J. Ma, D. S. Sanchez, B. Wang, A. Bansil, F. Chou, P. P. Shibayev, H. Lin, S. Jia and M. Z. Hasan, Science **349**, 613 (2015).

[6] B. Q. Lv, H. M. Weng, B. B. Fu, X. P. Wang, H. Miao, J. Ma, P. Richard, X. C. Huang, L. X. Zhao, G. F. Chen, Z. Fang, X. Dai, T. Qian and H. Ding, Phys. Rev. X **5**, 031013 (2015).

[7] S.-M. Huang, S.-Y. Xu, I. Belopolski, C.-C. Lee, G. Chang, B. Wang, N. Alidoust, G. Bian, M. Neupane, A. Bansil, H. Lin and M. Z. Hasan, Nat. Commun. **6**, 7373 (2015).

[8] H. Weng, C. Fang, Z. Fang, B. A. Bernevig and X. Dai, Phys. Rev. X **5**, 011029 (2015).

[9] C. Zhang, S.-Y. Xu, I. Belopolski, Z. Yuan, Z. Lin, B. Tong, N. Alidoust, C.-C. Lee, S.-M. Huang, H. Lin, M. Neupane, D. S. Sanchez, H. Zheng, G. Bian, J. Wang, C. Zhang, T. Neupert, M. Z. Hasan and S. Jia, arXiv:1503.02630 (2015).

[10] X. Huang, L. Zhao, Y. Long, P. Wang, D. Chen, Z. Yang, H. Liang, M. Xue, H. Weng, Z. Fang, X. Dai and G. Chen, Phys. Rev. X **5**, 031023 (2015).

[11] H. B. Nielsen and M. Ninomiya, Phys. Lett. B **130**, 389 (1983).

[12] J. Jerphagnon and D. S. Chemla, J. Chem. Phys. **65**, 1522 (1976).

[13] L. Alagna, T. Prosperi, S. Turchini, J. Goulon, A. Rogalev, C. Goulon-Ginet, C. R. Natoli, R. D. Peacock and B. Stewart, Phys. Rev. Lett. **80**, 4799 (1998).

[14] W. Voigt, Ann. Phys., Lpz. **18**, 651 (1905).

[15] F. I. Fedorov, Opt. Spectrosc. **6**, 237 (1959).

[16] E. L. Ivchenko, S. A. Permogorov and A. V. Selkin, JETP Lett. **27**, 24 (1978).

[17] E. L. Ivchenko, S. A. Permogorov and A. V. Selkin, Solid State Comm. **28**, 345 (1978).

[18] E. B. Graham and R. E. Raab, J. Opt. Soc. Am. A **13**, 1239 (1996).

[19] J. Goulon, N. Jaouen, A. Rogalev, F. Wilhelm, C. Goulon-Ginet, C. Brouder, Y. Joly, E. N. Ovchinnikova and V. E. Dmitrienko, J. Phys: Condens. Matter **19**, 156201 (2007).

[20] M. R. Norman, Phys. Rev. B **92**, 075113 (2015).

[21] Y. Joly, S. Di Matteo and O. Bunau, Eur. Phys. J. Special Topics **208**, 21 (2012).

[22] Y. Joly, Phys. Rev. B **63**, 125120 (2001). The FDMNES program can be downloaded at http://neel.cnrs.fr/spip.php?rubrique1007

[23] Y. Joly, O. Bunau, J. E. Lorenzo, R. M. Galera, S. Grenier and B. Thompson, J. Phys.: Conf. Ser. **190**, 012007 (2009).

[24] C. R. Natoli, Ch. Brouder, Ph. Sainctavit, J. Goulon, Ch. Goulon-Ginet and A. Rogalev, Eur. Phys. J. B **4**, 1 (1998).

[25] The results presented involve a convolution of the calculated spectrum with both a core hole (7.68 eV for the Ta L1 edge) and a photoelectron inverse lifetime, with the latter having a strong energy dependence (at high energies, 15 eV, with a midpoint value at 30 eV above the Fermi energy) [23]. Core hole widths tabulated in the FDMNES program are based on the x-ray literature [23].

[26] In Ref. 18, this intensity differential is due solely to the polar vector optical activity. This is not the case in the x-ray regime because of the $e^{iQ \cdot r_n}$ factors in Eq. 2.

[27] M. Hirayama, R. Okugawa, S. Ishibashi, S. Murakami and T. Miyake, Phys. Rev. Lett. **114**, 206401 (2015).

[28] L. E. Vorobev, E. L. Ivchenko, G. E. Pikus, I. I. Farbshtein, V. A. Shalygin and A. V. Shturbin, JETP Lett. **29**, 441 (1979).

[29] I. Sodemann and L. Fu, Phys. Rev. Lett. **115**, 216806 (2015).